

The DIST-Hand, an Anthropomorphic, Fully Sensorized Dexterous Gripper

Andrea Caffaz, Giuseppe Casalino, Giorgio Cannata, Giorgio Panin, Emanuele Massucco

DIST, University of Genoa
Via Opera Pia 13, 16145 Genova, Italy
{pino, caffaz, gpanin, cannata, lele2}@dist.unige.it

Abstract. This paper describes the features of the DIST-Hand dexterous gripper. The DIST-Hand is a mechanism constituted by fingers with 16 degrees of freedom and with a high degree of dexterity, designed for experiments in the area of grasping control, and Tele-manipulation. The current version of the gripper is lightweight and can be easily installed on various existing robots. Moreover, we present solutions concerning the control of a device oriented to the fine manipulation and the development of a novel prototype of an integrated force and tactile sensor based on conductive rubber.

1 Introduction

The development of robot dexterous grippers is a very challenging endeavor for many researchers. This paper briefly presents the development of the first prototype of the DIST-Hand dexterous gripper. The DIST-Hand is a 4-fingered mechanism with 16 degrees of freedom and with a high degree of dexterity. The main goal pursued during the development of the DIST-Hand has been that of designing a small and lightweight dexterous gripper with anthropomorphic kinematics, which could be easily installed even on small robot manipulators. This paper outlines the characteristics of the hand and discusses some general designing issues faced during the early stage of the development. In Section 2, the description of the finger as the elementary building block and the integrated DIST-Hand is provided. Then, in Section 3, we present the on-going design, development and testing procedures related with new integrated force and conductive rubber-based tactile sensors, while the following section describes the characteristic HW and SW of the multiprocessor, real-time based controller. Finally, some conclusions are drawn.

2 Design of the DIST-Hand Robot

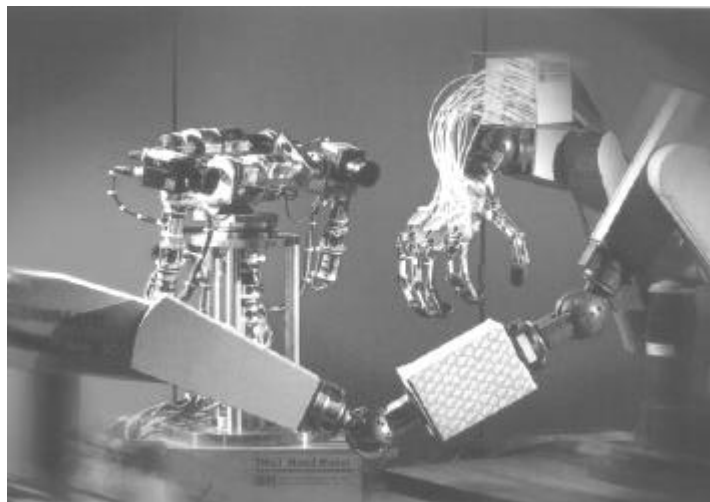


Fig. 1. The DIST-Hand dexterous gripper mounted on a PUMA 260 robot arm.

The basic element designed for the development of the DIST-Hand is a 4 degrees of freedom finger.

As the finger is the basic component of the hand in this paper we will mostly outline its characteristics and the methods followed during its design. As it will appear in the forthcoming discussion, during the design of the finger (and of the DIST-Hand as well) a particular attention has been given to the possibility of using whenever possible cheap off-the shelf components. This fact allowed to keep the costs and the time of development of the hand at very low levels. The following sub-sections illustrate the characteristics of the finger.

2.1 Finger Kinematics

The dimensions of the finger are close to that of a human one. The lengths of the various links, are listed in the following table

Link 1	Link 2	Link 3	Link 4
12 [mm]	42 [mm]	27.5 [mm]	28.5 [mm]

Fig. 2. Lengths of the various links

Each joint has a range of rotation which is larger than 90 deg and equivalent to that of a human hand. The most important aspect considered during the kinematic and mechanical design of the finger has been related to the need of ensuring adequate mobility to the mechanism. The first two joints of the finger have orthogonal axes; in particular the first axis allows to rotate the *distal plane* (i.e. the plane where the finger is bended during actual operations). The distal plane is orthogonal to the axes of the joints 2,3,4 and is a plane of symmetry of the finger. The distance between the first two axes has been kept as small as possible, to better emulate the finger kinematics.

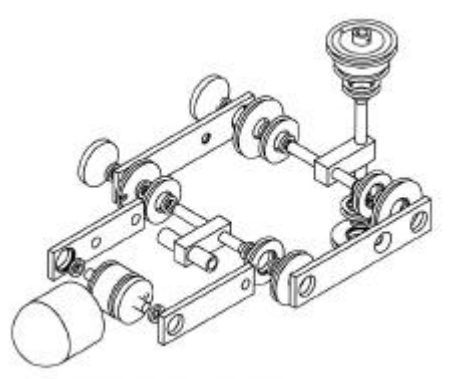


Fig. 3. The mechanical drawing of the finger

The kinematic structure of the finger is sketched in figure 3. All the idle pulleys are mounted on miniature ball bearings as well as the joint supports in order to reduce the friction effects. Each finger is actuated through 6 tendons ($\phi=0.4$ [mm]) made of polyester, routed through pulleys and driven by 5 DC motors. In particular, tendons 5 and 6 driving the first joint are actuated by a single motor and are passively pre-tensioned. The other 4 tendons are instead independently controlled by the remaining motors to drive the last 3 joints.

The actuation system has been carefully designed since it primarily affects the control performance of the robotic system. Three main problems have been addressed. Two of these have been mainly technological and involved basically the investigation of the most appropriate off-the-shelf components for the tendons, the tendons sheaths, and the motors.

The third problem has been instead mostly methodological and heavily influenced the final finger and hand design. This was the problem of designing the most appropriate routing of the tendons and dimensioning of the various pulleys. As outlined by many authors [1],[2] and particularly [3] the problem of routing the tendons in mechanical hands is critical at least for two main reasons. First of all not all the tendon routings are admissible in order to generate arbitrary joint torques since tendons can only exert unidirectional forces. Caratheodory theorem

establishes the minimum number of tendons needed, which is equal to $n+1$ where n is the number of joints [2], while Lee and Tsai [3] defined a procedure for the synthesis of admissible tendon routings.

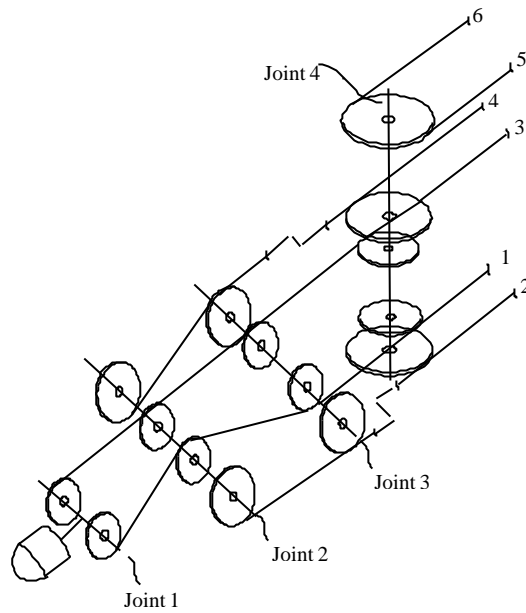


Fig. 4. Tendons routing of the DIST-Hand robot

Secondly, the mapping between tendon tensions (assumed to be massless and inelastic in the present discussion) and resultant joint torques is typically highly coupled thus making critical the problem of controlling the finger movements. These two aspects have been carefully taken into account during the DIST-Hand design. The tendons routing of the DIST-Hand is shown figure 4.

2.2 Finger Joint Sensors

The tendons and relative sheaths produce elastic perturbations in the position of the finger which make critical the control of the fingers' motions using position and velocity feedback directly from the motor axes.



Fig. 5. Hall-Effect Based position sensors mounted on the finger of the hand

Therefore, we have developed ad hoc rotation sensors mounted on each joint. Using these sensors it is possible to implement servo loops around the perturbations due to the elasticity and in part to friction. The sensor is based on the use of a solid state Hall effect transducer as proposed also in [4] and [5]. The basic sensor design is sketched in figure 6. The sensor is contactless therefore it does not affect the motion of the joints. Furthermore, it has a significant immunity to noise with respect to other transducers of comparable size (e.g. micro/mini potentiometers, encoders).

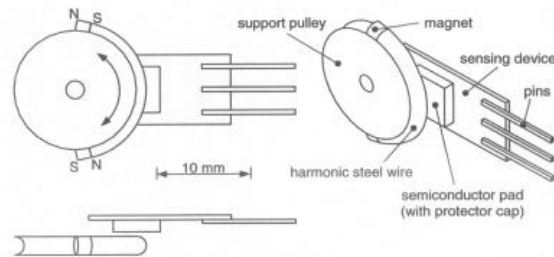


Fig.6. Sketch of the joint hall effect position sensor

The sensors output is a voltage $V=V(q)$, where q is the corresponding joint variable, with a S/N ratio of about 50dB, thus ensuring more than 8 bit resolution over a range of 110deg. The response curve of the sensor is mildly non linear, and strictly monotonically increasing.

2.3 Design of the Hand

The main goal of the DIST-Hand design has been that of developing an anthropomorphic gripper.

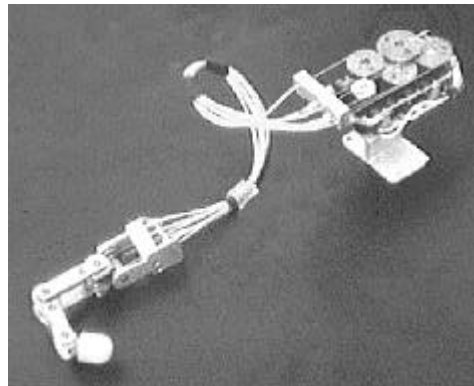


Fig. 7. The modular finger.

The finger modules described in the previous sections and shown in figure 7 represent the basic building blocks. A fundamental problem for developing a gripper with human like mobility is related with the fingers placement and in particular with the positioning of the thumb with respect to the palm.

The position of the fingers on the supporting palm (except for the thumb) has been defined accordingly with tabulated anthropomorphic data [6]. The position of the thumb has been instead studied using a custom kinematic simulation tool (figure 8). The simulator allowed to study the posture of the hand in response to various motion tasks involving the various fingers, using the techniques proposed in, [7];

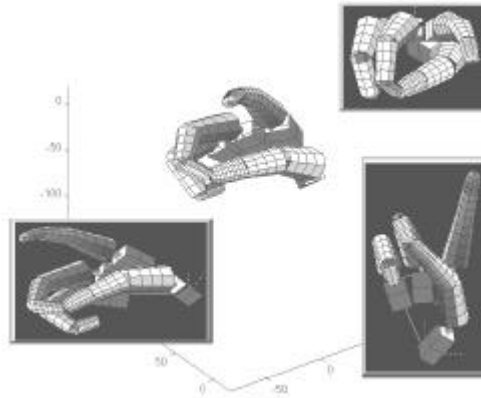


Fig. 8. The simulator to study the posture of the hand.



Fig 9. The motors pack of the DIST –Hand



Fig. 10. Comparison with a human hand

this analysis allowed to study the co-ordinated motion of two or more fingers, with particular emphasis on the problem of determining the posture of the hand when the thumb tip is in contact with the other finger-tips.

Finally the hand has been assembled and tendons have been routed to the motor package formed by 20 motors. The motors are low-cost DC motors with reduction gears able to produce an output torque of about 2 [Kg] cm and limited volume. The motor pack for a single finger has a volume lower than 100 [cm³]. The hand and the 20 motors weigh less than 10 N and can be easily fitted on various robot arm. Figure, shows the DIST-Hand installed on a PUMA 260 arm. The mechanical interfaces are very simple and not invasive for the supporting arm. Although the tendons sheaths somehow constrain the admissible motions of the PUMA wrist the mobility of the whole hand is adequately large.

The actual size of the DIST-Hand is comparable with that of an average human hand in figure 10. Finally the functionality of the hand has been proven in simple position controlled task which have been presented in [8].

3. Integrated force, tactile and slip detector device

State of art presents various kind of sensors to get information for fine manipulation[9] [10] [11] [12] [13].

To realize them two different techniques are usually used: superficial tactile sensor are built up using various kind of pressure transducers distributed on surface [9] [10] [13] and intrinsic force and torque sensor are usually realized using strain-gauges and estimating contact position [12]. Our idea is to integrate information coming from these two kind of sensors: an external tactile sensor will give data about contact position and the point of application of resultant forces, an intrinsic force sensor will work to determine the magnitude of the force as a three dimensional vector. This integration will lead to get enough information to realize a force based control loop for manipulation tasks.

3.1 force sensor

Has already been shown [12] that knowing the 6 components of force and torque

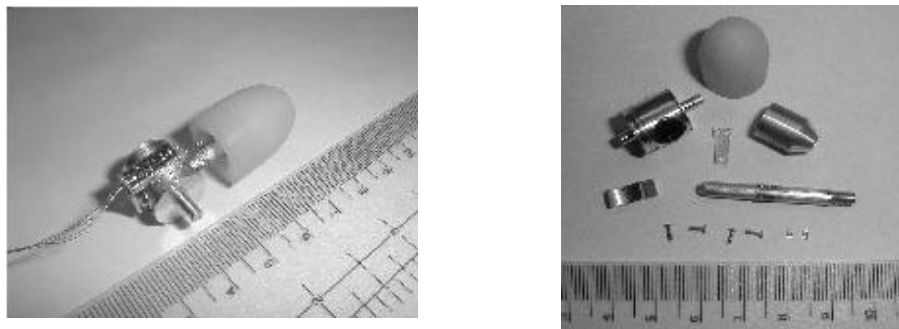


Fig. 11. Force sensor mounted on the finger tip of the Hand

measured respect to the end effector is possible to determine the coordinates of contact centroid and of the point of contact solving some particular algorithms, that give, under certain conditions, quite good, not always unique, approximated solutions.

An intrinsic force sensor able to determine the three component of the force applied on the fingertip was built to be mounted on DIST Hand robot, but the transducing core can be fit to any other structure.

By mean of the application of six strain-gauges in a three half-bridge configuration parallel to a reference resistor half-bridge ,we ensured to obtain temperature independent measurements and quite good signals also for very small deformation of the structure. To improve signal's quality four miniaturized amplifiers (one per finger) were built in order to be placed directly on the structure of DIST Hand.

Strain-gauges are placed in a particular way in order to guarantee the measure from each couple of gauges to be independent from the others.

Voltage measured on the gauges output are related to force components following the equation:

$$v = \mathbf{H} \cdot f \quad (1)$$

Where H_{ij} terms are calculated applying known force patterns, and the H matrix will be ideally diagonal. This means that H_{ij} terms are neglectable respect to the H_{ii} terms on the diagonal. Information about force application point is not directly obtainable from these data. To solve this problem in the most exact way there are the measures coming from a surface distributed tactile sensor able to better sense point(s) of contact(s), coordinates of centroid, normal forces, shape and orientation of the manipulated object. Integration of data coming from the two sensors will lead to determine all we need for fine manipulation.

3.2 Conductive rubber based tactile sensor

The using of conductive rubber in order to making tactile sensors represents a good economic and versatile technology [14][15].

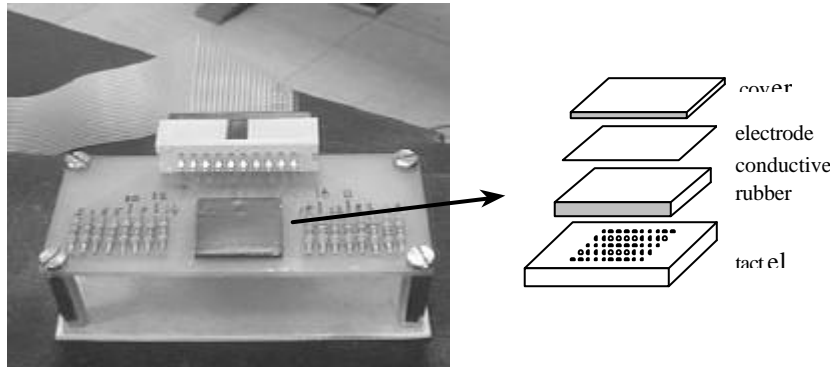


Fig.12. Conductive rubber based sensor

Moreover, the mechanical features, such as the compliance, make it able to be a good cover of the finger-tips [16].

This kind of silicone rubber are made of a drugged silicon rubber mixed with silver and graphit. The final product shows a little resistivity variation relating by a pressure; but it shows an important variation of the contact resistance depending on the applied force. In figure 12 the tactile sensor developed is showed.

All the measurements are related to a single rubber covered electrode. In the common set-up, every tactels are the cross between a raw and a column; in our case, any electric couple is not present. This allows to make an acquisition of the whole imagine of the sensor in the one-shot mode. In the other hand, in this case the number of connections rise from n to $n+1$ (where n is the number of tactels).

At this point, it seems necessary to spend some words about the main technique of data acquisition coming from a tactile sensor. Vision systems based on artificial retina have a strong analogy with tactile sensors. This is true for both the point of view of the hardware and the point of view of the data processing.

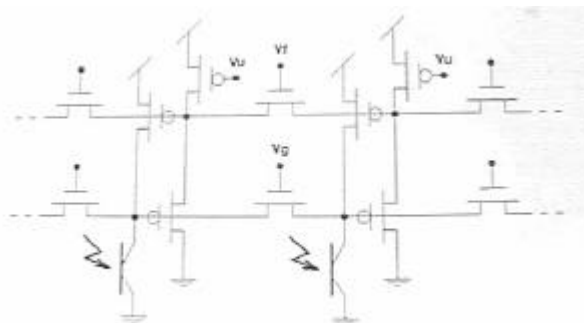


Fig.13. Silicon retina

Nowadays, a larger and larger number of analog circuits able to convert luminous signals in electric signals are developed by the VLSI techniques[17][18]. In figure 13, the scheme of the Silicon Retina designed by Kwabena Boahen [19] is showed.

This kind of devices allow to analyze the luminosity value in terms of pixel level, with respect the standard approach. It has been used an analog circuit. The operations are performed totally in parallel way. The imagines can be locally processed in real time on the same chip which manages the acquisition task. So, it leads to re-define the design of the same scheme, by replacing the photosensitive elements (pixel) with the piezoresistive elements (tactels). In this way, it becomes a tactile sensor, which is able to faster acquire tactile imagine.

This solution provides the local data acquisition and processing. The problem of the greater number of wires is not so important in this case. Indeed, the high speed of the whole sensor scanning is the most important feature.

Talking about the sensor, some tests have been conducted in order to rebuild the tactile imagine. The results are showed in figure 14.

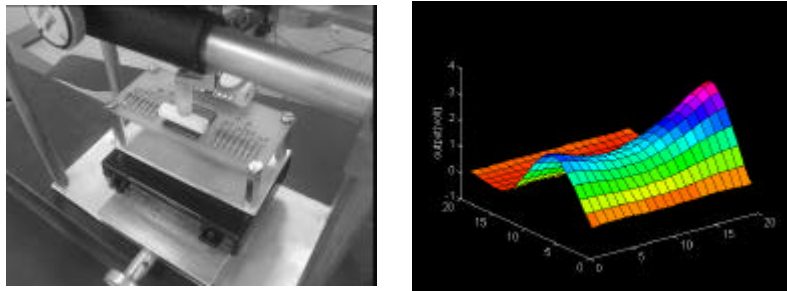


Fig. 14. Shape recognition.

A very interesting aspect of the conductive rubber is connected to the variation of his resistivity. Even if the variation of the contact resistance is ,of course, the main effect, the second one show an interesting characteristic showed in figure 15.

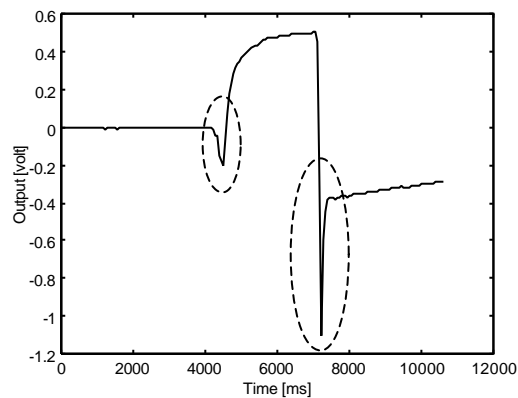


Fig. 15. Pulse stimulus (2.5 sec length).

By applying a constant force for a small time (in this case, about 2.5 seconds) we can see two spike in correspondence of the start and the end of the applied force, added to the decreasing of the resistance detected by the increasing of the voltage amplitude. In particular, a 100 ms spike can be always denoted in the presence of any kind of external force disturb. It depends on the increasing of the resistivity. The analyze of the structure of the conductive rubber can help us to understand this phenomena. The bond between the silionic rubber and the drug (graphite) is a physical bond. It means that the graphite particles are not chemically bonded with the rubber ones, but they are embedded in the rubber, as showed in figure 16.

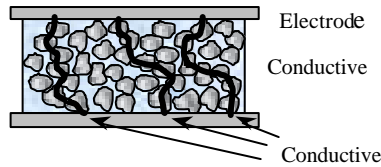


Fig.16. Conductive rubber

In the idle condition, a resistance R_0 is present between the electrodes applied on the rubber, through a number of conductive paths. Any kind of mechanical perturbation, connected to an impact on the sensor structure, will induce vibrations which will interrupt some conductive path as showed in figure 17.

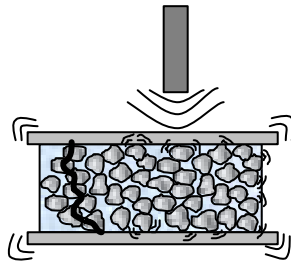


Figure 17. System submitted to vibrations.

In this way, the resistance R_0 increase rapidly. As the transitory time is finished, the system elasticity will trend to restore the idle condition and the resistance will be back to the R_0 value.

This hypothesis has been confirmed by making a macro model of the rubber-graphite system. As show in figure 18, some micro-spheres have been embedded inside a elastic membrane (the last one emulates the holding effect of the siliconic rubber).By perturbing the system, the same spike detected in the presence of the conductive rubber is denoted between the electrodes, as showed in figure 19.

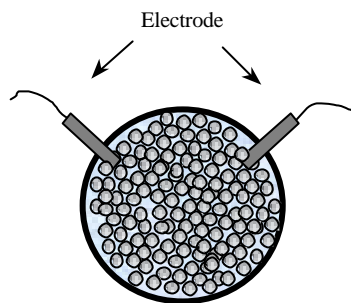


Fig. 18. Macro model

If weak force are applied, the spike is still present. A sequence of micro-impacts generates a sequence of spikes easy to detect. So, it could be used as contact trigger signal. Some vibrations (such a sequence of micro-impact) are induced in a scraping body; so, by the catch-snap phenomena [20][21], which happens during the slippage of a elastic material on rough surface.

This kind of vibration are strictly connected to the surface features of the material in exam, and they could be detected by the sensor. The vibration will generate a dense sequence of spike.

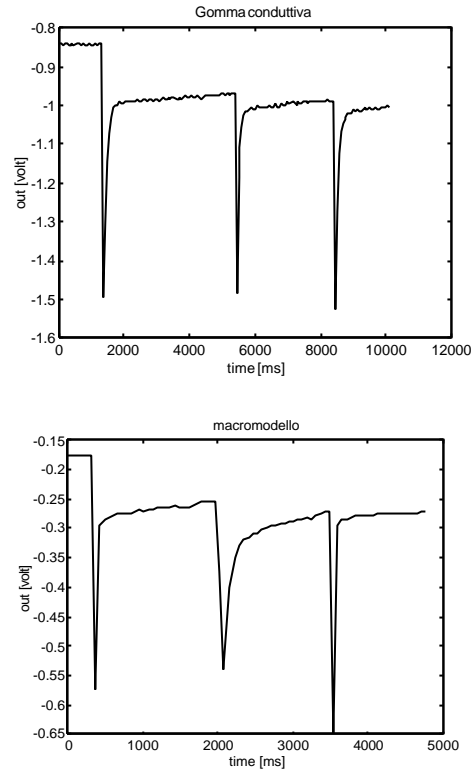


Fig.19. Comparison between Conductive rubber (Top) and Macro model (Bottom).

4 Control Issue

The present section describes some of the issues which have been considered and solved within the development of the control architecture for the whole hand.

For sake of brevity however, we will not enter here into accurate theoretical details, but simply summarize the main achievements. For more detailed theoretical discussions the reader may refer to [23 – 28] and, in particular to [29], where the controlling the grasped object motion, and interactions, during the hand manipulation is analyzed in full details.

4.1 Control Scheme

The mapping between tendon tensions \mathbf{f} and resultant joint torque \mathbf{t} is expressed by the following linear equation

$$\mathbf{t} = A^t \mathbf{f}; \quad A^t \in \tilde{\mathbf{A}}^{4 \times 6} \quad (7)$$

where A is called *structure matrix*. It is full rank, constant, and its entries are the radii of the pulleys through which each tendon is routed to generate any desired joint torque.

The relationship between the displacement of the tendons \mathbf{x}_q , as seen from the *joint* side, and the joint displacements \mathbf{q} , is expressed by the dual relationship

$$\mathbf{x}_q = A \mathbf{q} \quad (8)$$

From the *motors* side, the relationship between the displacement of the tendons \mathbf{x}_α , and the motor rotation \mathbf{a} , is expressed by

$$\mathbf{x}_\alpha = B \mathbf{a}; \quad B \in \tilde{\mathbf{A}}^{6 \times 5} \quad (9)$$

where the entries of full rank matrix B are still the radii of the pulleys mounted on the motors. Moreover, matrices A and B are such that:

$$\text{span}(A) \cap \text{span}(B) = \{0\} \quad (10)$$

From the above relationships, we can calculate the elongation of the tendons as:

$$\mathbf{D}\mathbf{x} = \mathbf{x}_q - \mathbf{x}_\alpha = \mathbf{A}\mathbf{q} - \mathbf{B}\mathbf{a} \quad (11)$$

If we consider the tensions vector \mathbf{f} , we can assume a linear relationship with the elongation vector:

$$\mathbf{f} = \mathbf{f}_0 - k\mathbf{D}\mathbf{x} \quad (12)$$

being $\mathbf{f}_0 \in \text{Ker}(A^t)$ the initial tension vector.

If we apply to the finger joints a vector \mathbf{c} of external torques (and assuming negligible finger masses), we must have

$$\mathbf{t} - \mathbf{c} = \mathbf{0} \quad (13)$$

That is due to (7), (11) and (12)

$$k A^t (\mathbf{A}\mathbf{q} - \mathbf{B}\mathbf{a}) = \mathbf{c} \quad (14)$$

Thus implying

$$\mathbf{q} = \mathbf{A}^+ \mathbf{B}\mathbf{a} - (1/k)(\mathbf{A}^t \mathbf{A})^{-1} \mathbf{c} \quad (15)$$

being \mathbf{A}^+ the left pseudoinverse of the matrix \mathbf{A} :

$$\mathbf{A}^+ = (\mathbf{A}^t \mathbf{A})^{-1} \mathbf{A}^t \quad (16)$$

We can comment expression (14) as follows

$$1) \text{span}(\mathbf{A}^+ \mathbf{B}) = \tilde{\mathbf{A}}^t$$

due to the full rank of both \mathbf{A} , \mathbf{B} and property (10)

2) we can consider the vector \mathbf{a} as an input to the system, while \mathbf{c} can be considered a “disturbance”, as in the following scheme:

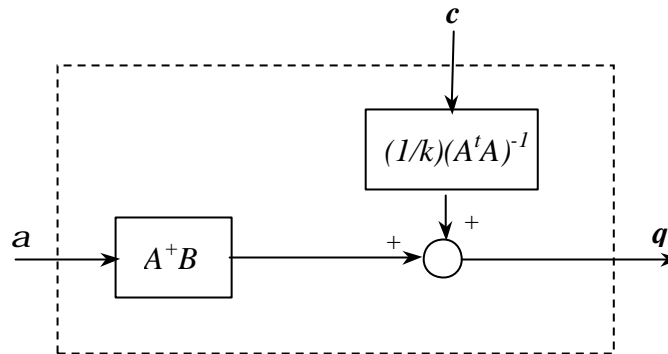


Fig.20. Motor to joint coordinates mapping

Now we can ask ourselves how to control this system, in order have \mathbf{a} tracking a desired reference vector $\bar{\mathbf{q}}$.

In case we had no disturbances this could be done in open loop by imposing \mathbf{a} as one of the solution of the equation.

$$\bar{\mathbf{q}} = A^+ B \mathbf{a} \quad (17)$$

or, equivalently:

$$(A^t A) \bar{\mathbf{q}} = A^t B \mathbf{a} \quad \hat{U} \quad A^t (A \mathbf{q} - B \mathbf{a}) = 0 \quad (18)$$

Thus, in order to impose the previous condition, we may to proceed in two distinct ways:

- 1) By looking at condition (17), as it is written in the left side of (17) itself, we can think to obtain a vector \mathbf{a} having *minimum norm* by left pseudo inverting $A^t B$; thus yielding

$$\bar{\mathbf{a}} = (A^t B)^\# (A^t A) \bar{\mathbf{q}} \quad (19)$$

That is

$$\bar{\mathbf{a}} = B^t A (A^t B B^t A)^{-1} (A^t A) \bar{\mathbf{q}} \quad (20)$$

Enough, this solution is always such that:

$$\bar{\mathbf{a}} \perp \text{Ker}(A^t B) \quad (20)$$

generally leading to non zero tendon elongations $\mathbf{D} \bar{\mathbf{x}}$ of the form

$$\mathbf{D} \bar{\mathbf{x}} = [I - B B^t A (A^t B B^t A)^{-1} A^t] A \bar{\mathbf{q}} \quad (21)$$

Nevertheless, such “non necessary” elongations $\mathbf{D} \bar{\mathbf{x}}$, and relevant tensions $k \mathbf{D} \bar{\mathbf{x}}$, do as not generate any motion, since $\mathbf{D} \bar{\mathbf{x}} \in \text{Ker}(A^t)$; in fact:

$$A^t \mathbf{D} \bar{\mathbf{x}} = A^t (A \bar{\mathbf{q}} - B \bar{\mathbf{a}}) = 0 \quad (22)$$

- 2) Instead, by looking at (17) as it appears written in the right side, we may also calculate another solution $\bar{\mathbf{a}}$, not with minimum norm, but however capable of avoiding the introduction of any additional elongation. Such a solution can be found by simply zeroing the second factor of (17) as it is written in the right side. Thus obtaining

$$\bar{\mathbf{a}} = B^+ A \bar{\mathbf{q}} = (B^t B)^{-1} B^t A \bar{\mathbf{q}} \quad (23)$$

With the adoption of such second possibility, the corresponding open loop control scheme consequently results as the one shown figure 21, where the additional signal

$$\mathbf{l} \in \text{Ker} A^t B \quad (24)$$

is purposely introduced for independently imposing a pretensioning effect to all the tendons, while not inducing any motion just as a consequence of (24).

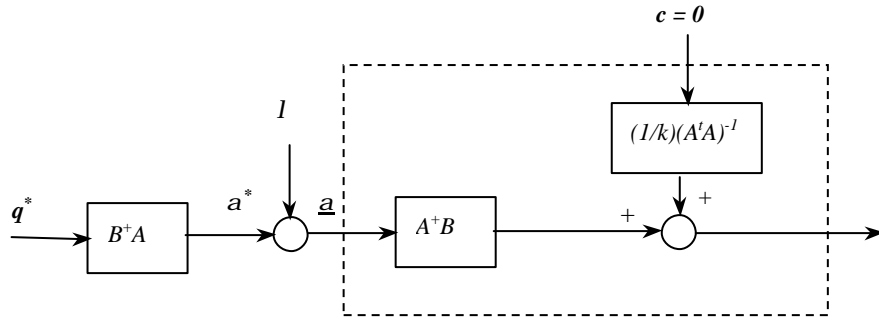


Fig.21. Open loop control scheme

More precisely the superimposed pretensioning effect results to be of the form:

$$Dx_0 = Bl \quad \hat{U} f_0 = k Bl \quad (25)$$

satisfying the condition (see (24))

$$A^T Dx_0 = A^T Bl = 0 \quad \hat{U} A^T f_0 = 0 \quad (26)$$

Naturally enough, being the above scheme an open loop one it can actually reject disturbances $c \neq 0$ only on the basis of an assumed "high value" for the tendons elastic coefficient k .

Such possible drawback can however be easily bypassed by transforming the previous open loop scheme into the closed loop one depicted in figure 22, via a suitable design of regulator R_1

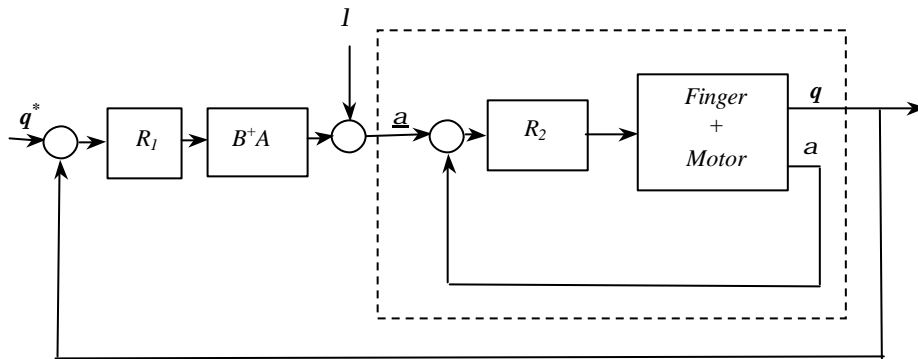


Fig. 22. Close loop control scheme.

Note how the above closed loop scheme is also comprehensive of "high gain" internal regulations R_2 closed around each one of the motors, accomplishing the task of guaranteeing $a @ \underline{a}$, as much as possible as required. Naturally enough, the angular measurements of a are provided by the potentiometers located in correspondence of each motor, while measurement of q are provided by the Hall-effect sensors mounted in correspondence of each joint.

Finally, as it concern the finger control at task level, an external loop is additionally closed around the scheme of figure 22.

More precisely, by denoting the control scheme of figure 22 with the terminology "Low level control" (LLC), then the external loop is denoted as "Medium level control" (MLC), and corresponds to the one depicted in the global scheme of figure 23.

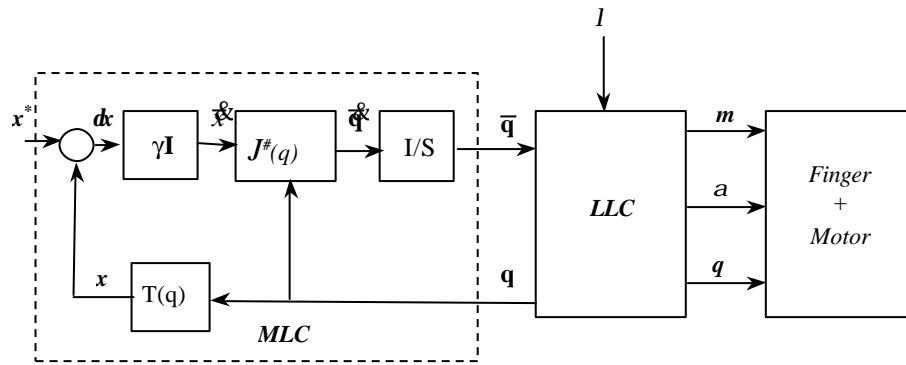


Fig. 23. Medium level and Low level control loop

As it can be easily seen, the external MLC scheme is designed in order to work as follows:

a) The Cartesian fingertip position x is on-line evaluated from the forth columns of the fingertip transformation matrix $T(q)$, b) The actual position x is compared with the reference one x^* and the resulting error δx is multiplied by a suitable gain matrix γI ; thus leading to a desired Cartesian velocity \dot{x} to be imposed to the fingertip, c) The desired cartesian velocity \dot{x} is then transformed in a corresponding desired joint velocity vector \dot{q} via pseudo inversion of the linear jacobian matrix of the finger, d) The so obtained joint velocity vector is then transformed, via integration, into the corresponding joint position reference signal \bar{q} for the LLC part of the scheme.

4.2 DIST-Hand Controller

The control hardware which has been adopted is VME based and it includes two Motorola 68040 based CPU boards and four IP modules for I/O purposes. The piggyback modules are two IP Precision ADC (sampling both hall sensors and potentiometers) and two DENSE-DAC (sending torque commands to the various motors).

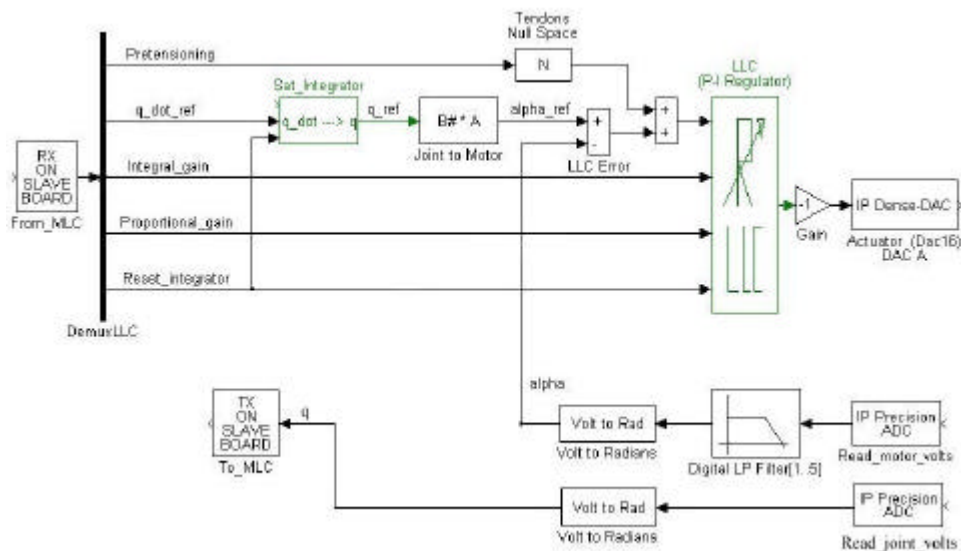


Fig.24. Low Level scheme in SIMULINK environment.

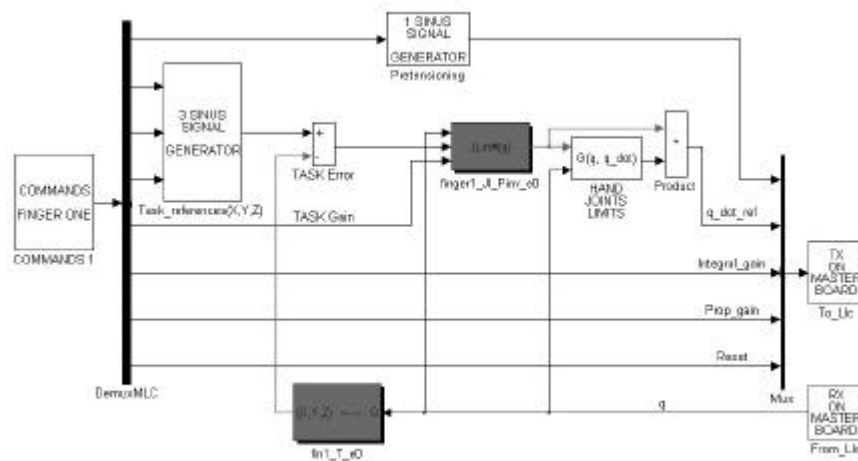


Fig.25. Medium Level Control scheme in SIMULINK environment.

The Simulink and Real Time Workshop MATLAB's Toolboxes jointly with the Wind River's TORNADO development environment have been used to design and implement the real controllers. In Figure 24 and it is shown the implementation of the Low Level Control and Medium Level Control within the SIMULINK environment.

The implementation of the Low Level Control includes the feedback and feedforward communication blocks (on the left), computational blocks for the joint to motor co-ordinates mapping and for the joint position proportional servoing loop (in the middle of the scheme). Finally we remark the presence of blocks containing the drivers for the I/O modules (on the right). The execution time concerning LLC is about (running on a MVME162 board) 1 msec.

In the Medium Level Scheme we remark the presence of the kinematic blocks (dark grey coloured) which compute the Jacobian matrix, the forward kinematic problem and implement the desired control law. Moreover there are blocks devoted to interface the controller with the human operator (on the left) and to communicate with the low-level control scheme (on the right). The interface is a simple tool which links a PC host (where a simulation of the scheme is running) with the real tasks execution on the target board. The communication channels exploits interrupts on the VME bus to speed-up the access made by the MLC board to critical memory regions implementing a mutual exclusion on a double buffer. The execution time of MLC (executed on a MVME167 board) is about 6 msec.

5. Conclusion

The design of the first prototype of the DIST-Hand dextrous gripper has been presented. The hand has a high degree of dexterity equivalent to that of other dextrous robot gripper already presented in the literature. However, some design issues followed during its development, to the best of the authors knowledge, have not been fully addressed in the existing literature. Furthermore the design of the DIST-Hand has been conceived to obtain a lightweight device which could be easily fitted on existing robot arms and operationally used for tele-operation experiments.

References

1. K. Salisbury, M. Mason, "Robot Hands and the Mechanics of Manipulation". MIT Press: Cambridge, MA. 1985.
2. R.N. Murray, Z. Li, S.S. Sastry, "A Mathematical Introduction to Robotic Manipulation". CRC Press. 1994.

3. J. Lee, L. Tsai, "The Structural Synthesis of Tendon-Driven Manipulators having Pseudotriangular Structure Matrix", *Int. Journ. of Robotic Research*, vol. 10, n. 3, 1991, pp. 255-262
4. C. Bonivento, C. Melchiorri, "Towards Dextrous Manipulation with the UB-Hand II", *Proc. 12th IFAC World Congress, Sydney (Australia), July 1993*.
5. S.C. Jacobsen, J.E. Wood, D.F. Knutti, K.B. Biggers, "The Utah-MIT Dextrous Hand: Work in Progress", *Int. Journ. of Robotic Research*, vol. 3, n. 4, 1983, pp. 21-50.
6. A. Farina, "Atlante di Anatomia Umana Descrittiva", *Recordati*. 1957 (in Italian)
7. M. Aicardi, G. Cannata, G. Casalino, "Task Space Robot Control: Convergence Analysis and Gravity Compensation Via Integral Feedback", *Proc. IEEE Conf. on Dec. and Control, Kobe (Japan), Dec. 1996*.
8. S. Bernieri, A. Caffaz, G. Cannata, G. Casalino, "The DIST-Hand Robot", *IROS '97 Conf. Video Proceedings, Grenoble (France), September 1997*.
9. R.S.Fearing. Tactile sensing mechanisms. *Int. J. of Robotics Research*, Vol.9 ,No.3, June 1990.
10. D. Johnston, P. Zhang, J. Hollerbach, S. Jacobsen. A full tactile sensing suite for dextrous robot hands and use in contact force control. *Proc. IEEE Int. Conf. Robotics and Automation*, 1996, pp.3222-3228.
11. A. Cicchetti, A. Eusebi, C. Melchiorri, G. Vassura. An intrinsic tactile force sensor for robotic manipulation. *ICAR 1995*.
12. A. Bicchi, J.K. Salisbury, D.L. Brock. Contact sensing from force measurements. *Int J. of Robotics Research*, Vol.12, No.3, June 1993.
13. E.G.M.Holweg, H.Hoeve, W.Jongkind-L.Marconi, C.Melchiorri, C:Bonivento. Slip detection by tactile sensors: algorithms and experimental results. *Proc. Of 1996 IEEE Int.Conf. Robotics and Automation*, April 1996.
14. R.A. Russell. Robot Tactile sensing.
15. A Survey of Robot Tactile sensing technology, *Int. J. of Robotics Reseach*, June1989.
16. K.B. Shimoga and A.A.Goldenberg "Soft materials for robotic fingers" *Proceeding of the IEEE International Conference of robotics and automation*. May 1992.
17. R.Douglas, M.Mahowald and C.Mead. Neuromorphic analogue VLSI. *Annu. Rev. Neurosci.* no.18, 1995.
18. G.Indiveri, J.Kramer and C. Koch. Neuromorphic vision chips: intelligent sensors for industrial applications.
19. K.A. Boahen and A.G. Andreou. A contrast sensitive silicon retina with reciproca synapses. *Advances in neural information processing systems*. Eds. IEEE, 1992, vol4, MIT Press.
20. R.Howe, M.Cutkosky. Sensing skin acceleration of slip and texture perception. *ICRA'89*, Scottsdale.
21. L.Marconi, C.Melchiorri. Incipient slip detection and control using a rubber-based tactile sensor. *IFAC'96 World Congr., San Francisco*, 1996.
22. G. Hirzinger, B. Brunner, J. Dietrich, J. Heindl, "Sensor-Based Space Robotics-Rotex and Its Telerobotic Features", *Trans. on Robotics and Automat.*, vol. 9, n. 5, Oct. 1993.
23. O. Khatib, "A Unified Approach for Motion and Force Control of Robot Manipulators: The Operational Space Approach", *IEEE Jour. Robotics and Automation*, vol. RA-3, n. 1, Feb. 1987.
24. M. Aicardi, A. Caiti, G. Cannata, G. Casalino, "Stability and Robustness Analysis of a two layered hierarchical architecture for the closed loop control of robots in the operational space", *Proc.1995 IEEE Int. Conf. of Robotics and Automation, Nagoya (J) May 1995*.
25. M. Aicardi, G. Cannata, G. Casalino "Task Level Position Control of Robots and Static Errors Compensation", *Proc. of the ISRAM'96-World Automation Congress, Montpellier (F), 1996*.
26. M. Aicardi, G. Caiti, G. Cannata, G. Casalino "Hierarchical Architecture for the Closed Loop Control of Robots in the Operational Space: Stability and Robustness Analysis", *Proc. of the Int. Conf. On Advanced Robotics 1995*.
27. T. Bozzo, G. Cannata, G. Casalino, A. Mautone and S. Reto "On the Design of Task Level Control Architecture for Complex Robotic Systems", *IV ECPD Conf. On Advanced Robotics, Moscow, Aug. 1998*.
28. T.Bozzo, A.Caffaz and S.Reto "On the Design of Task Level Control Architecture for The DIST Robotic Hand" *IAA'99 SOCO'99, Italy, June 1999*.
29. G.Casalino, G. Cannata, G. Panin, A. Caffaz "On a two-level hierarchical structure for the dynamic of multifingered manipulation", *Conference on Decision and Control, Sydney, Australia, Dec. 2000 (submitted)*.